

The host galaxy/AGN connection*.

Brightness profiles of early-type galaxies hosting Seyfert nuclei.

Alessandro Capetti¹ and Barbara Balmaverde¹

INAF - Osservatorio Astronomico di Torino, Strada Osservatorio 20, I-10025 Pino Torinese, Italy
e-mail: capetti@oato.inaf.it
e-mail: balmaverde@oato.inaf.it

Abstract. We recently presented evidence of a connection between the brightness profiles of nearby early-type galaxies and the properties of the AGN they host. The radio loudness of the AGN appears to be univocally related to the host’s brightness profile: radio-loud nuclei are only hosted by “core” galaxies while radio-quiet AGN are only found in “power-law” galaxies. We extend our analysis here to a sample of 42 nearby ($V_{\text{rec}} < 7000 \text{ km s}^{-1}$) Seyfert galaxies hosted by early-type galaxies. From the nuclear point of view, they show a large deficit of radio emission (at a given X-ray or narrow line luminosity) with respect to radio-loud AGN, conforming with their identification as radio-quiet AGN.

We used the available HST images to study their brightness profiles. Having excluded complex and highly nucleated galaxies, in the remaining 16 objects the brightness profiles can be successfully modeled with a Nuker law with a steep nuclear cusp characteristic of “power-law” galaxies (with logarithmic slope $\gamma = 0.51 - 1.07$). This result is what is expected for these radio-quiet AGN based on our previous findings, thus extending the validity of the connection between brightness profile and radio loudness to AGN of a far higher luminosity.

We explored the robustness of this result against a different choice of the analytic form for the brightness profiles, using a Sérsic law. In no object could we find evidence of a central light deficit with respect to a pure Sérsic model, the defining feature of “core” galaxies in this modeling framework. We conclude that, regardless of the modeling strategy, the dichotomy of AGN radio loudness can be univocally related to the host’s brightness profile. Our general results can be re-phrased as “radio-loud nuclei are hosted by core galaxies, while radio-quiet AGN are found in non-core galaxies”.

Key words. galaxies: active, galaxies: Seyfert, galaxies: bulges, galaxies: nuclei, galaxies: elliptical and lenticular, cD

1. Introduction.

The study of active galaxies attained a new role following recent developments in our understanding of the nuclear structure of galaxies and of its connection with the process of galactic formation and evolution. It is now clear that not only massive galaxies host a supermassive black hole (SMBH) in their centers but also that SMBH and host galaxies follow a common evolutionary path. This is suggested by the presence of tight relationships between the SMBH mass and the stellar velocity dispersion (Ferrarese & Merritt 2000; Gebhardt et al. 2000), as well as by the mass of the spheroidal component of their hosts (e.g. Marconi & Hunt 2003; Häring & Rix 2004). There is

also increasing evidence that, in the co-evolution of the SMBH/galaxy system, nuclear activity plays a major role in one of the many different forms known as active galactic nuclei (AGN). In fact, the energy liberated in the accretion process generates a feed-back process acting on the host galaxy (Di Matteo et al. 2005), e.g. suppressing the star formation in massive galaxies (Croton et al. 2006). Thus AGN obviously represent, on the one hand, our best tool for investigating formation and growth of SMBH. But on the other, nuclear activity also strongly influences galaxy evolution.

But, despite this breakthrough in our understanding of the SMBH/galaxy system, we still lack a clear picture of the connection between the properties of AGN and of their host galaxies. One of the crucial issues here is to explain the so-called AGN radio loudness dichotomy (e.g. Kellermann et al. 1994) which essentially corresponds to the ability of the central engine to produce highly collimated relativistic jets. Understanding the origin of this

Send offprint requests to: A. Capetti

* Based on observations obtained at the Space Telescope Science Institute, which is operated by the Association of Universities for Research in Astronomy, Incorporated, under NASA contract BAS 5-26555.

dichotomy is clearly important from the point of view of AGN physics. But, since it corresponds to different modes of energy transfer from the AGN into the host galaxy, it is also related to different feedback processes that couple nuclear activity and galaxy evolution. In this context, previous studies have not provided clear-cut answers. It is in fact well-established that spiral galaxies preferentially harbor radio-quiet AGN, but early-type galaxies can host both radio-loud and radio-quiet AGN. Similarly, radio-loud AGN are generally associated with the most massive SMBH as there is a median shift between the radio-quiet and radio-loud distribution, but both distributions are broad and overlap considerably (e.g. Dunlop et al. 2003).

In a series of three papers (Capetti & Balmaverde 2005, 2006; Balmaverde & Capetti 2006, hereafter CB05, CB06, BC06) we recently re-explored the classical issue of the connection between the multiwavelength properties of AGN in nearby early-type galaxies and the characteristics of their hosts. Early-type galaxies appear to be the critical class of objects, as they host AGN of both classes of radio loudness. Starting from an initial sample of 332 galaxies, we selected 116 AGN candidates (requiring the detection of a radio source with a flux limit of ~ 1 mJy, as measured from 5 GHz VLA observations). In CB05 we analyzed the 65 objects with available archival HST images where a classification into “core” and “power-law” galaxies was possible for 51 objects, distinguishing them on the basis of the nuclear slope of their brightness profiles following the modeling scheme proposed by Lauer et al. (1995).

We used HST and Chandra data to isolate the nuclear emission of these galaxies in the optical and X-ray bands, thus enabling us (once combined with the radio data) to study the multiwavelength behavior of their nuclei. The properties of the nuclei hosted by the 29 “core” galaxies were presented in BC06. “Core” galaxies invariably host a radio-loud nucleus, with a median radio loudness of $\text{Log } R = 3.6$ and an X-ray based radio loudness parameter of $\text{Log } R_X = -1.3$. In CB06 we discussed the properties of the nuclei of the 22 “power-law” galaxies. They show a substantial excess of optical and X-ray emission with respect to “core” galaxies at the same level of radio luminosity. Conversely, their radio loudness parameters, $\text{Log } R \sim 1.6$ and $\text{Log } R_X \sim -3.3$, are similar to those measured e.g. in Seyfert galaxies selected from the Palomar survey (Ho et al. 1997) for which $\text{Log } R \sim 1.9$ and $\text{Log } R_X \sim -3.6$ (Panessa et al. 2007).

As already noted by Ho & Peng (2001), if we were to adopt the classical dividing line between radio-loud and radio-quiet objects introduced by Kellermann et al. (1994), i.e. at $\text{Log } R = 1$, a substantial fraction of Seyfert and “power-law” galaxies should be considered as radio-loud. However, the recent work by Panessa et al. shows that at low luminosities (with respect to high-luminosity QSO for which the radio loudness definition was originally proposed) AGN still separate into two different populations of radio loudness, but the two classes are optimally distinguished by using $\text{Log } R \sim 2.4$ and $\text{Log } R_X \sim -2.8$ as

thresholds. The difference between these values and the traditional separation drawn at $\text{Log } R = 1$ is most likely an indication of a luminosity evolution of the level of radio loudness.

Adopting this definition, the radio loudness of AGN hosted by early-type galaxies can be univocally related to the host’s brightness profile: radio-loud AGN are only hosted by “core” galaxies, while radio-quiet AGN are found only in “power-law” galaxies.

Since the brightness profile is determined by the galaxy’s evolution through its merger history (e.g. Faber et al. 1997; Ryden et al. 2001; Khochfar & Burkert 2003), our results suggest that the same process sets the AGN flavor. In this scenario, the black holes hosted by the merging galaxies rapidly sink toward the center of the newly formed object, setting its nuclear configuration, described by e.g. the total mass, spin, mass ratio, or separation of the SMBHs. These parameters are most likely at the origin of the different levels of the AGN radio loudness. For example, it has been proposed that a “core” galaxy is the result of (at least) one major merger and that the core formation is related to the dynamical effects of the binary black holes on the stellar component (e.g. Milosavljević et al. 2002; Ravindranath et al. 2002). From the AGN point of view, Wilson & Colbert (1995) suggested that a radio-loud source can form only after the coalescence of two SMBH of similar (high) mass, forming a highly spinning nuclear object, from which the energy necessary to launch a relativistic jet can be extracted. In this situation (the merging of two large galaxies of similar mass), the expected outcome is a massive “core” galaxy in line with our results. The connection of the radio loudness with the host’s brightness profile might open a new path toward understanding the origin of the radio-loud/radio-quiet AGN dichotomy, and it provide us with a further tool for exploring the co-evolution of galaxies and super-massive black holes. A better understanding of this issue would put us in the position of relating the manifestation of nuclear activity in a given galaxy with its formation history.

We present here the analysis of the brightness profiles of a sample of 42 nearby ($cz \leq 7000 \text{ km s}^{-1}$) Seyfert galaxies hosted by early-type galaxies. This study is motivated by the extremely low nuclear luminosity of the objects we selected in CB05, a characteristic of volume-limited surveys in which the rare high-luminosity objects tend to be under-represented. Indeed the objects we considered previously extend only, with just a few exceptions, to an X-ray luminosity of up to $\sim 10^{41} \text{ erg s}^{-1}$. This lead us to mainly explore a regime of a very low level of AGN activity. The nature of these low luminosity objects and their relationship with brighter AGN is still a matter of much debate (e.g. Chiaberge et al. 2005; Maoz 2007). It is thus important to establish whether the results we obtained for these weakly active galaxies, relating the properties of the AGN with those of their host galaxy, can be extended to objects more representative of the overall AGN population. Considering Seyfert galaxies we indeed extend the

coverage up to an X-ray luminosity of $\sim 10^{43}$ erg s $^{-1}$. The analysis of a sample of Seyfert galaxies thus represents a significant step forward for the study of the AGN/host galaxy connection. In particular this study will enable us to test the prediction based on our previous findings that these radio-quiet AGN should be hosted by “power-law” galaxies.

With respect to the initial series of 3 papers we include here a full modeling of the brightness profiles also with a Sérsic (1968) model. There are several reasons suggesting this approach. First of all, Graham et al. (2003) argue that a Sérsic model provides a better characterization of the brightness profiles of early-type galaxies, in particular considering their large-scale curvature (in a Log-Log space) and, furthermore, that a Sérsic fit can reproduce the brightness profiles of dwarf ellipticals (Graham & Guzmán 2003) with very low values for the nuclear slope. They also suggest a new definition of “core” galaxy as the class of objects showing a light deficit toward the center with respect to the Sérsic law (Trujillo et al. 2004). Recently, an analysis of the brightness profiles of 100 early-type galaxies in the Virgo cluster (the Virgo Cluster Survey, VCS) has been presented by Ferrarese et al. (2006). This work provides us with a useful benchmark for interpreting our results within this modeling scheme not previously available in the literature. On the other hand, Lauer et al. (2006) question these results, arguing that Sérsic models are not a good representation of the central regions of the surface brightness profiles of early-type galaxies. Since the situation is far from settled and there is significant controversy on this issue, we preferred to use both analytic forms. Quite reassuringly, we show that our results are independent of the fitting scheme and we recover a unique correspondence between the host’s brightness profile and the AGN properties.

The structure of the paper is as follows. In Sect. 2 we describe the sample studied and in Sect. 3 we present the HST images used to derive the surface brightness profiles that are modeled using both a Nuker and a Sérsic model. The multiwavelength properties of our sample are discussed in Sect. 4 where we show that they all conform to the definition of radio-quiet AGNs. In Sect. 5 we summarize and discuss our results.

We adopt a Hubble constant $H_0 = 75$ km s $^{-1}$ Mpc $^{-1}$.

2. Sample selection and basic data

A detailed description of the selection criteria of the sample analyzed in this paper can be found in Mulchaey et al. (1996) and Nagar et al. (1999). Briefly, Mulchaey et al. selected their sample of Seyfert galaxies with early-type hosts from the catalogue of Hewitt & Burbidge (1991), J. P. Huchra (1989, private communication) and Veron-Cetty & Veron (1991), restricting it to a range of magnitude and recessional velocity for which morphological classification is complete and reliable, i.e. total magnitude $m_V \leq 14.5$ and recessional velocity $cz \leq 7000$ km s $^{-1}$.

High-quality VLA radio observation of the galaxies of the sample were presented by Nagar et al. (1999), with the further requirement of a declination greater than $\delta = -41^\circ$. Three objects later found to satisfy the selection criterion (namely NGC 7743, Mrk 335, and Mrk 612) were added to the original list by Nagar et al. Since the radio data are a crucial ingredient for our study, we restrict the analysis to this group of 42 galaxies¹ that form our final sample.

In Table 1 we report the basic data of these Seyfert galaxies: name, Seyfert type, recession velocity (corrected from Local Group infall into Virgo), total K-band magnitude from 2MASS, the radio flux at 3.6 and 20 cm from Nagar et al. (1999) (when the radio-source is extended, we also give the radio-core flux) and the stellar velocity dispersion from the HYPERLEDA database (available for 26 sources).

In Fig. 1 we compare the K band absolute magnitudes and the estimated black-hole masses² for the sample of Seyfert galaxies against the two sub-samples of early-type galaxies we analyzed in CB05, separated into “power-law” and “core” galaxies. The luminosity distributions of Seyfert hosts and of “power-law” galaxies match closely, with the same median value of $M_K = -23.8$, while they are both fainter (by about 1 mag) than “core” galaxies for which the median magnitude is $M_K = -24.8$. Nonetheless a large overlap between the three classes is found in the region $-23.5 < M_K < -25$. A slightly different result is found when comparing the distribution of black-hole masses: Seyfert, “power-law”, and “core” galaxies have median values of $\text{Log } M_{BH} = 7.6, 8.0, \text{ and } 8.5$ respectively. But again, there is a broad region of overlap. We note that stellar velocity dispersion measurements are available for only 26 Seyfert galaxies of our sample and, in general, they are affected by substantial uncertainties due to the dilution of the absorption lines caused by the active nucleus. The comparison between the M_{BH} distributions should be then treated with some caution.

3. Surface brightness profile analysis

We explored the properties of the surface brightness profiles of the galaxies of the sample retrieving images from the HST archive, available for all but 4 objects. All data were calibrated by the standard on the fly re-processing (OTFR) system. The resulting images are presented in Figs. 2 through 3. The HST images of the sample of Seyfert galaxies were obtained in different instruments and filters as reported in Table 2, but most images were obtained using the broad-band filter F606W (R band) on the WFPC2 or the F160W filter (H band) on the NICMOS.

We derived a one-dimensional surface-brightness profile by fitting elliptical isophotes to the images using the IRAF task ‘ellipse’ (Jedrzejewski 1987). This step of the

¹ We also excluded MCG-2-27-9 since it was not observed by Nagar et al.

² Estimated using the relationship with the stellar velocity dispersion in the form given by Tremaine et al. (2002).

Table 1. Basic properties of the Seyfert sample

Name	Host Type	Sy Type	V	m_K	$F_{3.6\text{cm}}$	$F_{20\text{cm}}$	$F_{\text{core}3.6\text{cm}}$	$F_{\text{core}20\text{cm}}$	σ
MRK 335	S0/a	1	7698	10.059 ± 0.030	2	6.8			
MRK 348	SA0/a	2	4624	10.097 ± 0.047	238.0	302.2			118
NGC 424	SB0/a	2	2154	9.129 ± 0.021	13.1	23.9	12.2	23.9	
NGC 526A	S0 pec?	2	5466	10.436 ± 0.050	5.0	10.5	5.0	5.9	
NGC 513	S0?	2	5510	9.914 ± 0.020	...	41.2	...	4.2	152
MRK 359	SB0 pec	1.5	5125	10.461 ± 0.026	0.5	2.4			
MRK 1157	SB0/a	2	4674	10.063 ± 0.028	4.9	25.7			95
MRK 573	SAB0	2	5139	10.385 ± 0.030	1.8	14.3			123
NGC 788	SA0/a	2	3806	9.071 ± 0.025	0.7	2.9			140
ESO 417-G6	SA0/a?	2	4699	10.237 ± 0.043	1.0	3.1			
MRK 1066	SB0	2	3733	9.793 ± 0.023	16.4	96.3	4.8	95.3	105
MRK 607	S0/a	2	2612	9.359 ± 0.029	1.3	3.7			116
MRK 612	SBa	2	6053	10.650 ± 0.036	2.2	8.2			
NGC 1358	SAB0/a	2	3924	8.948 ± 0.032	0.9	3.4			173
NGC 1386	Sa/S0	2	610	8.066 ± 0.014	9.1	28.8			120
ESO 362-G8	S0?	2	4520	9.568 ± 0.024	0.8	2.7	0.4	2.7	
ESO 362-G18	S0/a	1.5	3550	10.025 ± 0.033	2.8	6			
NGC 2110	SA0/SBa?	2	2064	8.144 ± 0.019	130.1	289.0	81.2	289.0	220
MRK 3	E2 pec	2	4248	8.970 ± 0.019	79.0	1060	50.1	1060	269
MRK 620	SAB0/a,SBab	2	2049	8.480 ± 0.020	10.2	52.0	7.6	52.0	124
MRK 6	SAB0+,Sa	1.5	6101	9.560 ± 0.017	30	253			
MRK 10	SAb,SBbc	1.2	8968	10.345 ± 0.038	...	0.5			143 ^a
MRK 622	S0 pec	2	7094	11.078 ± 0.064	1.7	6.0			100
MCG -5-23-16	S0	2	2294	9.349 ± 0.021	...	11.0			210 ^a
MRK 1239	compact	1.5	5684	9.603 ± 0.015	7.9	56.5			263 ^a
NGC 3081	SAB0/a	2	2243	8.910 ± 0.028	1.0	3.5			
NGC 3516	SB0,SB0/a	1.2	2902	8.512 ± 0.027	4.1	9.4			235
NGC 4074	S0 pec	2	6875	10.566 ± 0.028	0.8	2.0			192
NGC 4117	S0	2	1143	10.047 ± 0.031	<0.1	2.2			95
NGC 4253	SB0/a,SBa	1.5	4038	9.839 ± 0.022	8.6	39.3			
ESO 323-G77	SAB0	1.2	4352	8.802 ± 0.017	1.3	31.9			
NGC 4968	SAB0	2	2858	9.481 ± 0.037	6.5	32.3			
MCG -6-30-15	E-S0	1.2	2168	9.582 ± 0.017	0.9	4			162 ^a
NGC 5252	S0	2	6773	9.768 ± 0.037	9.3	17.2	7.9	13.5	190
MRK 270	SAB0	2	3152	9.974 ± 0.028	3.1	13.9			148
NGC 5273	SA0	1.5	1316	8.665 ± 0.024	0.6	2.4			79
IC 4329A	S0	1.2	4660	8.805 ± 0.013	10.7	60			235 ^a
NGC 5548	SA0/a,Sa	1.2	5310	9.387 ± 0.019	3.1	23	3.1	6	48 ^a
ESO 512-G20	SB0	1	3309	10.447 ± 0.049	1.2	3.6			
IC 5169	SAB0 pec	2	2943	9.776 ± 0.015	3.7	17.6			
NGC 7465	SB0	2	2046	9.542 ± 0.021	1.2	6.0			
NGC 7743	SB0	2	1725	8.418 ± 0.028	0.9	5.3			83

Column description: (1) Name, (2) Host type (3) Seyfert type (4) recession velocity in km s^{-1} corrected for LG infall onto Virgo from HYPERLEDA, (5) total K band galaxy's magnitude from 2MASS, (6) total radio-flux [mJy] at 3.6 cm, (7) total radio-flux [mJy] at 20 cm, (8) nuclear radio-flux[mJy] at 3.6 cm, (9) nuclear radio-flux[mJy] at 20 cm, (10) stellar velocity dispersion in km s^{-1} from Nelson & Whittle (1995) or from ^a HYPERLEDA.

analysis is often compromised by the presence of complex structures that cannot be reproduced with an ellipse fitting (this is the case for most optical images). The 16 galaxies discarded at this stage are marked in Table 2 as 'complex'.

As explained in the Introduction, we performed a fit on these profiles by using both a Nuker law (Lauer et al. 1995) (see Sect. 3.1) and a Sérsic (1968) model (see Sect. 3.2). We followed the same approach as in CB05, e.g. minimizing the residuals between the data and the models convolved with the appropriate point spread function, pro-

duced with the TINYTIM software. Given the widespread presence of bright nuclear point sources, we preferred to include an unresolved nuclear source in the fit, while in CB05 we excluded the central regions from the fit in the case of a nucleated galaxy.

3.1. Nuker fit to the brightness profiles.

On the surface brightness profiles we performed a fit with a Nuker law in the form

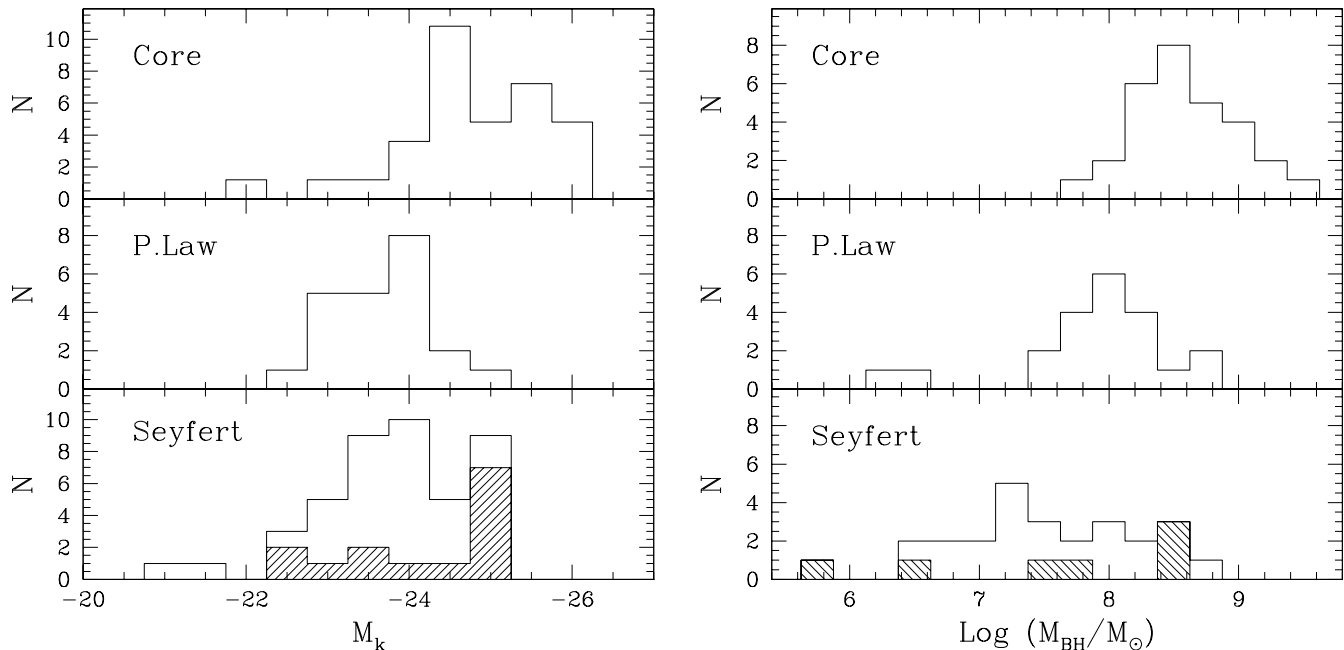


Fig. 1. Distribution of absolute magnitudes M_K (left panel) and of black hole masses M_{BH} (right panel) compared for the two sub-samples of the early-type galaxies we analyzed in CB05 (separated into “core” and “power-law” galaxies) and for the present sample of Seyfert galaxies. The shaded region in the bottom panels marks the contribution of type I Seyfert.

$$I(r) = I_b 2^{(\beta-\gamma)/\alpha} \left(\frac{r_b}{r}\right)^\gamma \left[1 + \left(\frac{r}{r_b}\right)^\alpha\right]^{(\gamma-\beta)/\alpha}.$$

The parameter β measures the slope of the outer region of the brightness profile, r_b is the break radius (corresponding to a brightness I_b), where the profile flattens to a smaller slope measured by the parameter γ and α sets the sharpness of the transition between the inner and outer profile.

In Fig. 4 we superposed the best fit with a Nuker law to the actual data in the top panel, while the lower panel presents the residuals for the 21 galaxies for which an ellipse fitting was possible. In Table 2 we report the best-fit parameters. In 6 objects, all type I Seyfert, the presence of bright nuclei prevents us to explore the properties of their host galaxies in the innermost regions: only a large scale emission tail, well described by a single power-law, can be seen in these objects (marked as ‘nucleated’ in Tab. 2³).

Nonetheless there are 3 exceptions to this general behavior among Seyfert 1, namely NGC 3516, ESO 323-G77, NGC 5273, all observed with NICMOS in the infrared band. Here a clear change in the slope (with a difference between the slope of the outer and inner power-law is $\beta - \gamma > \sim 0.8$) of the brightness profile occurs at sufficiently large radius (with $r_b \sim 1''.3 - 2''.4$), in a region where the nuclear emission provides a negligible contribution.

³ For one nucleated galaxy, Mrk 335, the optical image is saturated at the center and no brightness profile is given.

Conversely, the nuclear point sources in Sy 2, although often present, are not as prominent as in Sy 1 and this allows us to study in more detail this sub-sample. Eleven Seyfert 2 galaxies can be reproduced with a Nuker law with a well resolved break radius (we conservatively adopt a minimum value for the break radius of $r_b \geq 0''.2$ to consider it sufficiently resolved to yield an estimate of the cusp slope γ). It two cases (namely NGC 4968 and NGC 3081) we were only able to set an upper limit to the break radius of $0''.2$.

Summarizing, the Nuker law provides an accurate description for 16 galaxies of the sample, 3 Sy 1 and 13 Sy 2. The typical amplitude of the largest residuals of the modeling are in the range of 0.01-0.03 dex. Only in the two objects (namely NGC 4968 and NGC 3081) the brightness profile shows a ‘bump’ at relatively large radii and a Nuker fit is possible only excluding this region. The nuclear cusps are reproduced with a slope in the range $\gamma = 0.51 - 1.07$, typical of “power-law” galaxies.

3.2. Sérsic fit to the brightness profiles.

Leaving aside the 6 nucleated galaxies, we performed a fit on the remaining 16 galaxies of the sample using a Sérsic (1968) law for the brightness distribution given by the expression

$$I(r) = I_e \exp \left\{ -b_n \left[\left(\frac{r}{r_e} \right)^{1/n} - 1 \right] \right\},$$

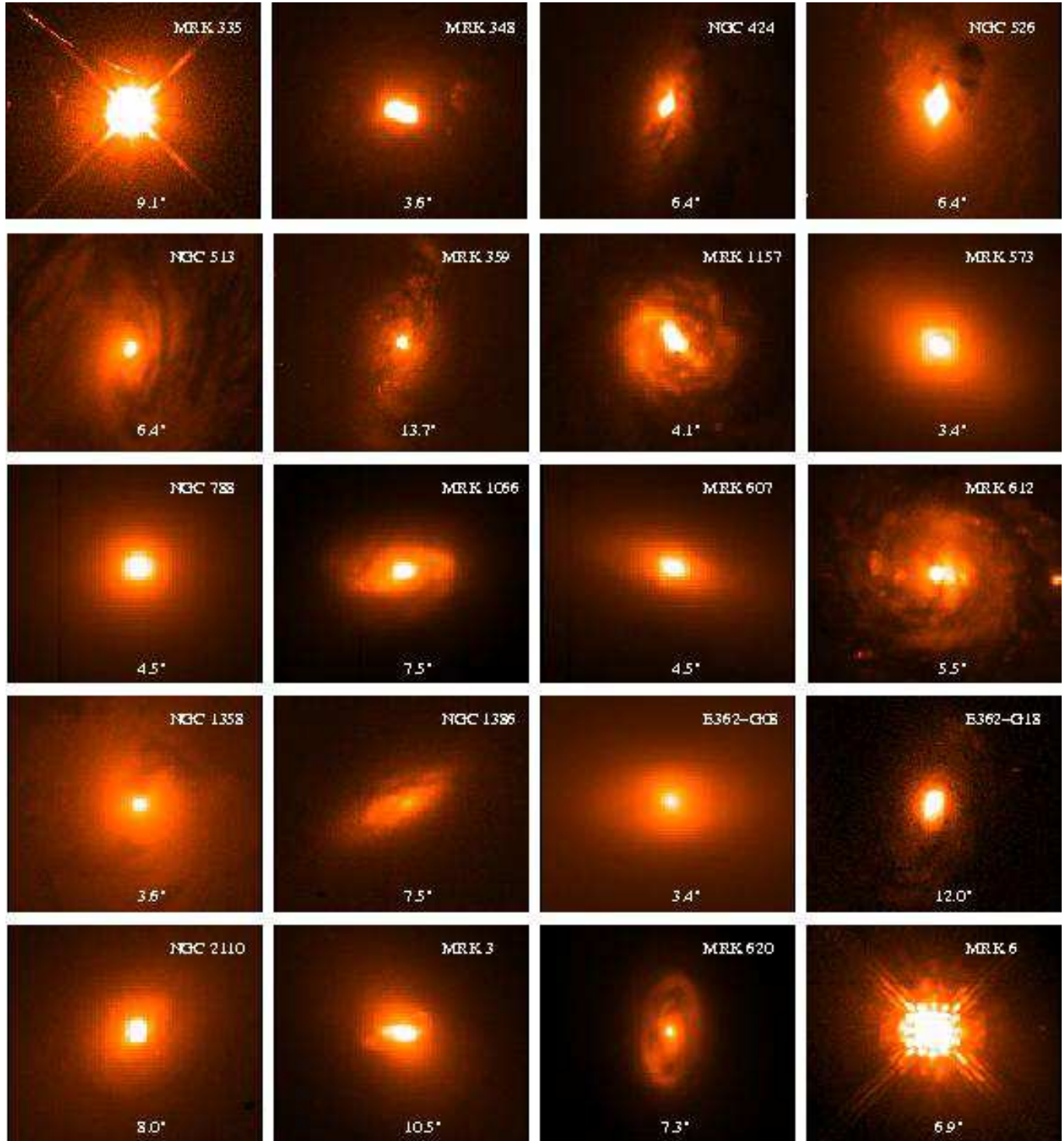


Fig. 2. HST images of the Seyfert galaxies of the sample. The image size is given in the bottom. The instrument/filter combination is reported in Table 2.

where n is the shape parameter, I_e is the intensity at the half-light radius r_e . The quantity b_n is a function of n , and is defined so that r_e is the radius enclosing half the light of the galaxy model; it can be approximated by $b_n \approx 1.9992n - 0.3271$, for $1 \lesssim n \lesssim 10$ (see e.g. Graham et al. 2003).

The fitting results are presented graphically in Fig. 5, and tabulated in Table 3. All profiles are well fitted with a Sérsic law, with an accuracy similar to that obtained with a Nuker law. In several cases, however, the behavior at large radii, while still substantially well reproduced

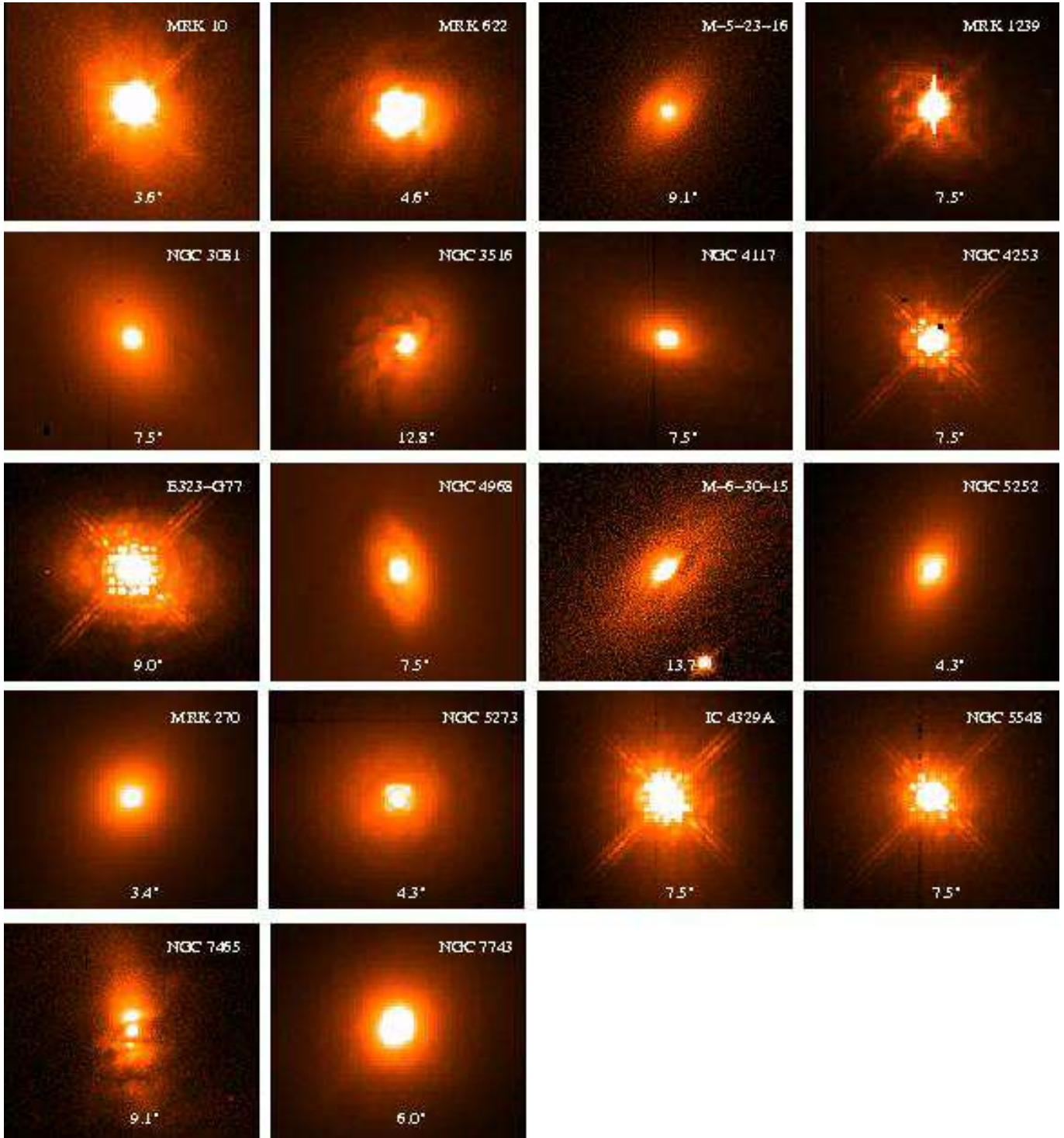


Fig. 3. HST images of the Seyfert galaxies of the sample. The image size is given in the bottom. The instrument/filter combination is reported in Table 2.

by the model, shows residuals in the form of large scale fluctuations with a typical amplitude of 0.05 dex.

The defining element of a core-Sérsic galaxy is the presence of a light deficit with respect to the Sérsic law (Trujillo et al. 2004). This should manifest itself in a characteristic S-shaped pattern in the residuals when using a

pure Sérsic model, with a central deficit and a larger scale excess. In no case we see such a signature.

Nonetheless, since our sample is formed by galaxies which are at larger distances than those considered by us in CB05 (the limit on the recession velocity for this sample is 3000 km s^{-1} , while the median here is 2900 km s^{-1}) and

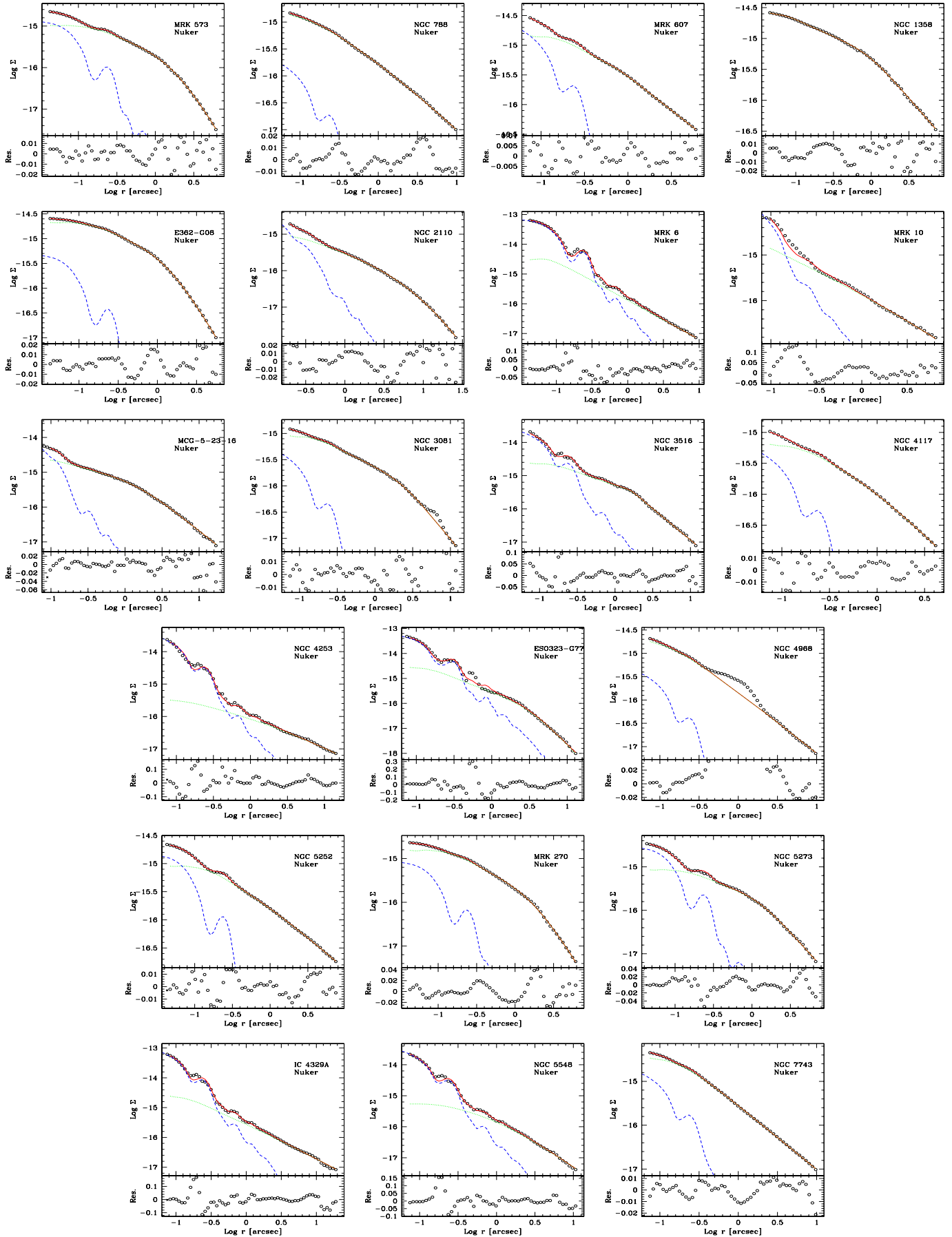


Fig. 4. Fit (solid line) to the observed brightness profiles (in $\text{erg s}^{-1} \text{cm}^{-2} \text{\AA}^{-1}$ units) obtained with a Nuker law. The

Table 2. Nuker parameters for the Seyfert sample.

Name	Sy Type	HST Image	α	β	γ	r_b	μ_b
MRK 335	1	WFPC2/F606W	Saturated				
MRK 348	2	WFPC2/F606W	Complex				
NGC 424	2	WFPC2/F606W	Complex				
NGC 526A	1.9	WFPC2/F606W	Complex				
NGC 513	2	WFPC2/F606W	Complex				
MRK 359	1.5	WFPC2/F606W	Complex				
MRK 1157	2	WFPC2/F606W	Complex				
MRK 573	2	NIC1/F160W	1.93	3.14	0.62	1.74	-16.10
NGC 788	2	NIC2/F160W	0.67	1.39	0.51	0.26	-15.19
ESO 417-G06	2	Unobserved					
MRK 1066	2	NIC2/F160W	Complex				
MRK 607	2	NIC2/F160W	6.27	1.15	0.73	0.81	-15.44
MRK 612	2	WFPC2/F606W	Complex				
NGC 1358	2	WFPC2/F606W	3.11	1.41	0.52	0.92	-15.29
NGC 1386	2	NIC2/F160W	Complex				
ESO 362-G08	2	NIC1/F160W	2.14	2.67	0.60	1.33	-15.60
ESO 362-G18	1.5	WFPC2/F547M	Complex				
NGC 2110	2	NIC3/F160W	1.04	3.43	0.64	10.80	-16.91
MRK 3	2	WFPC2/F814W	Complex				
MRK 620	2	NIC2/F160W	Complex				
MRK 6	1.5	NIC1/F160W	Nucleated				
MRK 10	1.2	WFPC2/F606W	Nucleated				
MRK 622	2	WFPC2/F606W	Complex				
MCG -5-23-16	2	WFPC2/F791W	2.06	1.70	0.53	1.48	-15.44
MRK 1239	1.5	WFPC2/F606W	Complex				
NGC 3081	2	NIC2/F160W	2.64	1.79	0.66	2.27	-15.99
NGC 3516	1.2	NIC2/F160W	23.5	1.67	0.92	1.62	-15.46
NGC 4074	2	Unobserved					
NGC 4117	2	NIC2/F160W	1.31	1.50	0.53	0.55	-15.72
NGC 4253	1.5	NIC2/F160W	Nucleated				
ESO 323-G77	1.2	NIC2/POL0L	2.24	3.24	1.07	3.39	-16.39
NGC 4968	2	NIC2/F160W	-	1.34	-	< 0.2	-
MCG -6-30-15	1.2	WFPC2/F791W	Complex				
NGC 5252	1.9	NIC1/F160W	1.26	1.16	0.66	0.74	-15.68
MRK 270	2	NIC1/F160W	2.05	2.87	0.80	1.74	-16.06
NGC 5273	1.5	NIC1/F160W	2.90	1.97	0.63	1.27	-15.86
IC 4329A	1.2	NIC2/F160W	Nucleated				
NGC 5548	1.2	NIC2/F160W	Nucleated				
ESO 512-G20	1	Unobserved					
IC 5169	2	Unobserved					
NGC 7465	2	WFPC2/F791W	Complex				
NGC 7743	2	NIC2/F160W	-	1.46	-	< 0.2	-

Notes: the break radius r_b is given in arcsec; the brightness at the break radius is in a Log scale in $\text{erg s}^{-1} \text{cm}^{-2} \text{\AA}^{-1}$ units.

by Ferrarese et al. (2006) there is the possibility that genuine “core” galaxies might be misclassified as pure Sérsic due to an insufficient physical resolution of the images. However, the median core size measured for the sample of nearby early-type galaxies studied in CB05 is ~ 200 pc, similar to the values found by Faber et al. (1997) et al. (250 pc) and by Ferrarese et al. (2006) in the Virgo survey (150 pc), considering only “core” galaxies. Given the distances to each of the 16 galaxies considered here, a scale of 200 pc corresponds to $0''.46 - 2''.8$, with a median of $1''.1$, far larger than the HST resolution.

The presence of point sources also limit our ability to see shallow cores. We then estimated the size of the region significantly compromised by the presence of the nucleus

as the radius r_{nuc} at which it produces a contribution of 10 % of the galaxy’s starlight. The value of r_{nuc} is always smaller than 70 pc, with a median of only 25 pc, indicating that in general the nuclear emission does not hamper the detection of a stellar core with a typical size of 200 pc.

We conclude that the presence of a light deficit extended over the typical core size seen in other samples studied in the literature would have been easily seen in the light profiles presented here, despite the larger distances of the galaxies of the sample and the presence of prominent nuclear point sources. The lack of such signature indicates that the Seyferts hosts can be considered as pure-Sérsic galaxies, without evidence for the presence of core-Sérsic galaxies in this sample.

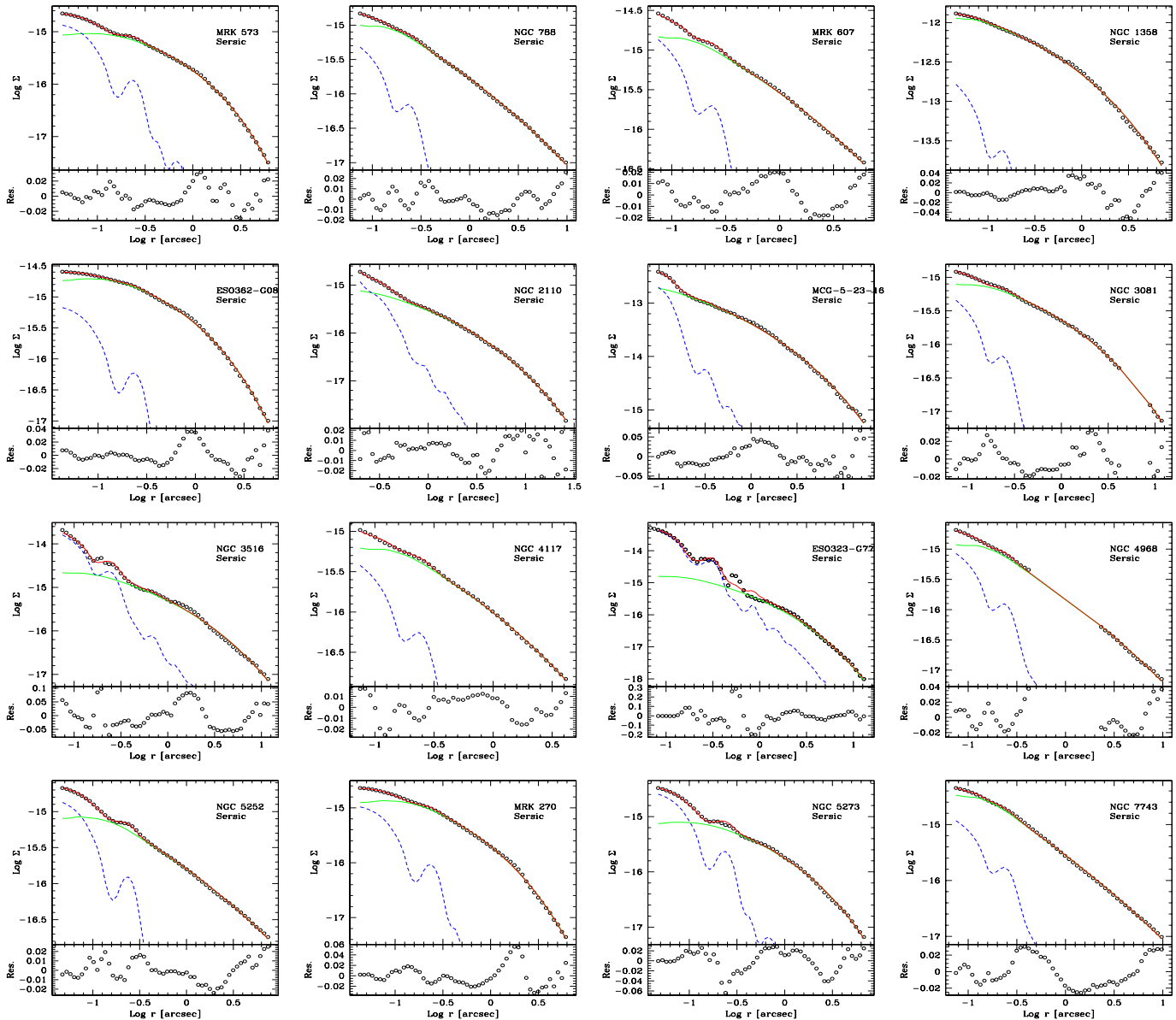


Fig. 5. Fit (solid line) to the observed brightness profiles (in $\text{erg s}^{-1} \text{cm}^{-2} \text{\AA}^{-1}$ units) obtained with a Sérsic law, having excluded complex and nucleated sources. The dotted and dashed lines represent the contribution of the galaxies light and nuclear sources respectively. Residuals of the fit are given in the bottom panel.

4. Multiwavelength properties of the Seyfert nuclei

To study the nuclear properties of our Seyfert sample we searched the literature for published emission-line and X-ray nuclear luminosities. With respect to our previous works, we will not use the information on the optical nuclei. In fact, in the case of Seyfert 2 galaxies that form the majority of this sample, it is well established that their optical emission is substantially affected by nuclear obscuration. Conversely, observational evidence suggests that the X-ray (once corrected for absorption) and narrow emission line luminosities provide sound orientation-independent measures of the intrinsic luminosity of the nuclei of AGNs (e.g. Mulchaey et al. 1994).

The X-ray data available in the literature are tabulated in Table 4. The X-ray measurements are very heterogeneous, based on observations of different satellites (ASCA, ROSAT BeppoSax, Einstein, XMM, and Chandra) obtained over more than 20 years. Although these observations have a large range of resolution and sensitivity, Seyfert galaxies are associated to sufficiently bright X-ray sources that they can be measured at a sufficient level of accuracy for our purposes even with X-ray telescopes of past generations. We only discarded ROSAT data for the Seyfert 2 galaxies since in its energy range (0.1-2.5 keV) the thermal host emission, and not the highly absorbed non-thermal nucleus, is likely to be the dominant component at these low energies. When more than one measurement was available, we referred the more recent mea-

Table 4. X-ray and optical spectral information

Name	X-ray data summary				Line information	
	Observation date	Instrument	F(2-10 keV)	Ref.	F _[OIII]	Ref.
MRK 335	1993Dec	ASCA	9.2E-12	(23)	2.0E-13	(30)
MRK 348	1995Aug	ASCA	4.80E-12	(2)	2.8E-13	(12)
NGC 424	2002Feb/2001Dec	Chandra/XMM	1.60E-12	(3)	2.4E-13	(18)
NGC 526A	1995Nov	ASCA	3.44E-11	(20)	3.1E-13	(12)
NGC 513					1.5E-13	(12)
MRK 359	2000Jul	XMM	1.26E-11	(24)	1.1E-13	(12)
MRK 1157					2.1E-13	(12)
MRK 573	1979Jul	Einstein	5.6E-13	(4)	3.5E-12	(4)
NGC 788			4.6e-12		2.9E-13	(12)
ESO 417-G6					1.1E-13	(12)
MRK 1066	1997Aug	ASCA	3.60E-13	(5)	1.7E-13	(12)
MRK 607					2.4E-13	(12)
MRK 612					1.8E-13	(16)
NGC 1358	1980Aug	Einstein	1.40E-13	(6)	1.1E-13	(12)
NGC 1386	1995Jan	ASCA	3.88E-13	(7)	7.9E-13	(13)
ESO 362-G8					3.1E-13	(12)
ESO 362-G18					3.4E-13	(12)
NGC 2110	1997Oct	BeppoSAX	3.00E-11	(8)	1.8E-13	(14)
MRK 3	1997Apr	BeppoSAX	6.50E-12	(9)	2.8E-12	(17)
MRK 620	1996Oct	ASCA	1.20E-13	(7)	1.1E-13	(12)
MRK 6	1997Apr	ASCA	1.0E-11	(25)	1.48E-12	(29)
MRK 10	1990/1991	ROSAT	4.82E-12	(28)	1.4E-13	(32)
MRK 622					3.0E-14	(12)
MCG -5-23-16	1998Apr	BeppoSAX	10.50E-11	(10)	1.7E-13	(19)
MRK 1239	1990/1991	ROSAT	4.03E-14	(28)	2.1E-13	(12)
NGC 3081	1996Dec	BeppoSAX	13.30E-13	(11)	4.9E-13	(15)
NGC 3516	1994Apr	ASCA	7.80E-11	(23)	4.8E-13	(32)
NGC 4074					7.0E-14	(12)
NGC 4117	1997Dec	ASCA	3.71E-12	(21)	7.0E-14	(12)
NGC 4253	1990Dec	ROSAT	1.33E-11	(27)	4.3E-13	(12)
ESO 323-G77					1.8E-13	(12)
NGC 4968	1994Feb	ASCA	3.56E-12	(20)	2.1E-13	(19)
MCG -6-30-15	1994Jul	ASCA	4.6E-11	(23)	3.6E-15	(16)
NGC 5252	1994Jan	ASCA	5.72E-12	(20)	2.7E-14	(1)
MRK 270	1979Apr	Einstein	<2.85E-11	(22)	2.7E-13	(12)
NGC 5273	1990/1991	ROSAT	1.0E-13	(26)	1.2E-13	(19)
IC 4329A	1993Aug	ASCA	7.8E-11	(23)	2.7E-13	(12)
NGC 5548	1993Jul	ASCA	4.3E-11	(23)	1.1E-13	(31)
ESO 512-G20					6.0E-15	(12)
IC 5169					1.0E-14	(12)
NGC 7465					2.9E-13	(12)
NGC 7743	1998Dec	ASCA	7.30E-14	(7)	5.7E-14	(13)

Column description: (1) optical name, (2) observation date, (3) Instrument, (4) X-ray flux in the 2-10 keV band, (5) reference for the X-ray analysis (see below for the list), (6) [O III] emission line flux [$\text{erg cm}^{-2} \text{s}^{-1}$], (7) reference for the line flux.

References: (1)Gu et al. (2006), (2) Awaki et al. (2000), (3) Matt et al. (2003), (4) Ulvestad & Wilson (1983), (5) Levenson et al. (2001), (6) Fabbiano et al. (1992), (7) Terashima et al. (2002), (8) Malaguti et al. (1999), (9) Cappi et al. (1999), (10) Risaliti et al. (2002), (11) Maiolino et al. (1998), (12)Mulchaey et al. (1996), (13)Storchi Bergmann & Pastoriza (1989), (14)Shuder (1980), (15)Durret & Bergeron (1986), (16)Shuder & Osterbrock (1981), (17)Koski (1978), (18)Murayama & Taniguchi (1998), (19)Ferruit et al. (2000), (20)Turner et al. (1997), (21) Terashima et al. (2000), (22)Kriss et al. (1980), (23)Reynolds (1997), (24)O'Brien et al. (2001), (25)Feldmeier et al. (1999), (26)Roberts & Warwick (2000), (27)Molendi et al. (1993), (28)Pfefferkorn et al. (2001), (29)Whittle et al. (1988), (30)Kuraszkiewicz et al. (2000), (31)Wilson et al. (1989), (32)Whittle (1992)

surement or the one at higher resolution. We rescaled the X-ray luminosities (see Table 5) to our adopted distance and converted to the 2-10 keV band, using the published power-law index.

From the literature we also collected the [OIII] emission line fluxes. They are given in Table 4, which includes the relative references, while the derived emission line luminosities can be found in Table 5.

Table 3. Sérsic parameters for the Seyfert sample.

Name	$\text{Log } I_e$	r_e	n	$\gamma_{0.1}$
MRK 573	-16.15	1.81	1.85	0.38
NGC 788	-18.23	49.26	6.22	0.72
MRK 607	-17.90	48.16	5.58	0.64
NGC 1358	-13.82	7.14	2.83	0.42
ESO 362-G08	-15.85	1.85	1.93	0.40
NGC 2110	-16.76	9.04	2.71	0.36
MCG -5-23-16	-14.72	9.37	3.20	0.46
NGC 3081	-16.85	8.35	2.77	0.38
NGC 3516	-16.28	4.80	2.72	0.45
NGC 4117	-17.50	9.75	4.39	0.68
ESO 323-G77	-16.16	2.54	2.40	0.48
NGC 4968	-18.19	35.63	6.95	0.84
NGC 5252	-18.43	80.61	5.99	0.63
MRK 270	-16.16	1.92	2.31	0.51
NGC 5273	-16.49	3.20	2.28	0.40
NGC 7743	-18.09	36.69	9.10	1.02

Notes: the effective radius r_e is given in arcsec, while I_e is in a Log scale in $\text{erg s}^{-1} \text{cm}^{-2} \text{\AA}^{-1}$ units. $\gamma_{0.1}$ is the corresponding logarithmic slope of the brightness profile evaluated at $0''.1$.

As for the X-ray data, line luminosities are obtained with different methods (imaging and spectrophotometry) and apertures. Nonetheless, since the [O III] emission tends to be strongly nucleary concentrated (see e.g. Mulchaey et al. 1996) it does not strongly depend on aperture. Furthermore, our analysis is based on orders of magnitude effects and as such it is quite stable against changes within a factor of a few in the line (or X-ray) luminosities.

In the following we compare the nuclear properties of these Seyfert galaxies with the samples of early-type galaxies we studied in CB05, BC06, and CB06. In Fig.6 (on the left) we compared X-ray and radio luminosities⁴. Seyfert galaxies are located well above the correlation defined by low luminosity radio-galaxies (LLRG) and “core” galaxies (by a factor $\sim 10 - 10^4$). At the lower luminosities they show a behavior similar to the radio-quiet “power-law” galaxies, but they extend the coverage by a factor of 100 toward higher radio luminosities and by a factor of 1000 in X-ray and line luminosities. Furthermore, our Seyfert sample, including only early-type hosts, follows a trend in the L_r vs L_x plane similar to the Seyfert galaxies from the Palomar studied by Panessa et al. (2007).

In CB06 we showed that radio-loud and radio-quiet AGN, i.e. LLRG/“core” and “power-law” galaxies, are well separated also when comparing radio and [O III] emission line luminosity, leading to the definition of a spectroscopic radio loudness parameter, $R_{[\text{OIII}]}$. Fig.6 (right panel) shows that Seyfert galaxies have a large excess also of line-emission (at a given radio-core luminosity) with respect to radio-loud objects.

The distributions of the radio loudness parameters R_X (based on the ratio between radio luminosity at 5 GHz

⁴ NGC 3516 AKA UGC 6153 is part both of the Seyfert and “power-law” samples. We mark its representative point in Fig.6 only as Seyfert galaxy.

Table 5. Multiwavelength luminosity of the Seyfert galaxies

Name	$\text{Log } \nu L_r$	$\text{Log } L_x$	$\text{Log } L_{[\text{OIII}]}$	M_K
MRK 335	38.10	43.06	41.40	-25.00
MRK 348	39.73	42.34	41.10	-23.85
NGC 424	37.78	41.20	40.37	-23.16
NGC 526A	38.20	43.34	41.29	-23.88
NGC 513	35.51	–	40.98	-24.42
MRK 359	37.14	42.85	40.79	-23.71
MRK 1157	38.06	–	40.99	-23.91
MRK 573	37.70	41.50	42.29	-23.79
NGC 788	37.03	42.15	40.95	-24.46
ESO 417-G6	37.37	–	40.71	-23.75
MRK 1066	37.85	41.03	40.70	-23.69
MRK 607	36.97	–	40.54	-23.35
MRK 612	37.93	–	41.14	-23.88
NGC 1358	37.17	40.66	40.55	-24.65
NGC 1386	36.56	39.49	39.79	-21.49
ESO 362-G8	36.94	–	41.13	-24.33
ESO 362-G18	37.57	–	40.96	-23.35
NGC 2110	38.56	42.43	40.21	-24.05
MRK 3	38.98	42.40	42.03	-24.80
MRK 620	37.53	40.03	39.99	-23.70
MRK 6	39.07	42.90	42.07	-24.99
MRK 10	37.63	42.91	41.38	-25.04
MRK 622	37.96	–	40.50	-23.80
MCG -5-23-16	34.75	43.07	40.28	-23.08
MRK 1239	38.43	40.44	41.16	-24.79
NGC 3081	36.73	41.15	40.72	-23.47
NGC 3516	37.56	43.14	40.93	-24.43
NGC 4074	37.60	–	40.85	-24.25
NGC 4117	35.14	41.01	39.29	-20.87
NGC 4253	38.17	42.66	41.17	-23.82
ESO 323-G77	37.42	–	40.86	-25.02
NGC 4968	37.75	41.79	40.56	-23.42
MCG -6-30-15	36.65	42.66	38.55	-22.72
NGC 5252	38.58	42.74	40.42	-25.01
MRK 270	37.51	42.78	40.75	-23.14
NGC 5273	36.04	39.56	39.64	-22.56
IC 4329A	38.39	43.55	41.09	-25.16
NGC 5548	37.97	43.41	40.82	-24.86
ESO 512-G20	37.14	–	39.14	-22.78
IC 5169	37.53	–	39.26	-23.19
NGC 7465	36.73	–	40.41	-22.64
NGC 7743	36.45	39.66	39.56	-23.39

Column description: (1) name, (2) nuclear radio luminosity (5GHz), $\text{Log} [\text{erg s}^{-1}]$, (3) intrinsic nuclear X-ray luminosity (2-10 keV), $\text{Log} [\text{erg s}^{-1}]$, (4) [O III] emission line luminosity, $\text{Log} [\text{erg s}^{-1}]$, (5) total K band absolute magnitude.

and the 2-10 keV X-ray luminosity, following the definition introduced by Terashima & Wilson (2003))⁵ and $R_{[\text{OIII}]}$ estimated from the ratio of [O III] luminosity and radio power for the different samples are shown in Fig. 7. Seyfert galaxies have both radio loudness parameters significantly lower than those derived for “power-law” galaxies, and, a fortiori, of the LLRG and “core” galaxies. With only 3 exceptions, Seyfert galaxies show value of X-ray radio

⁵ having converted the radio luminosity at 3.6 cm adopting a radio spectral index of $\alpha = 1$.

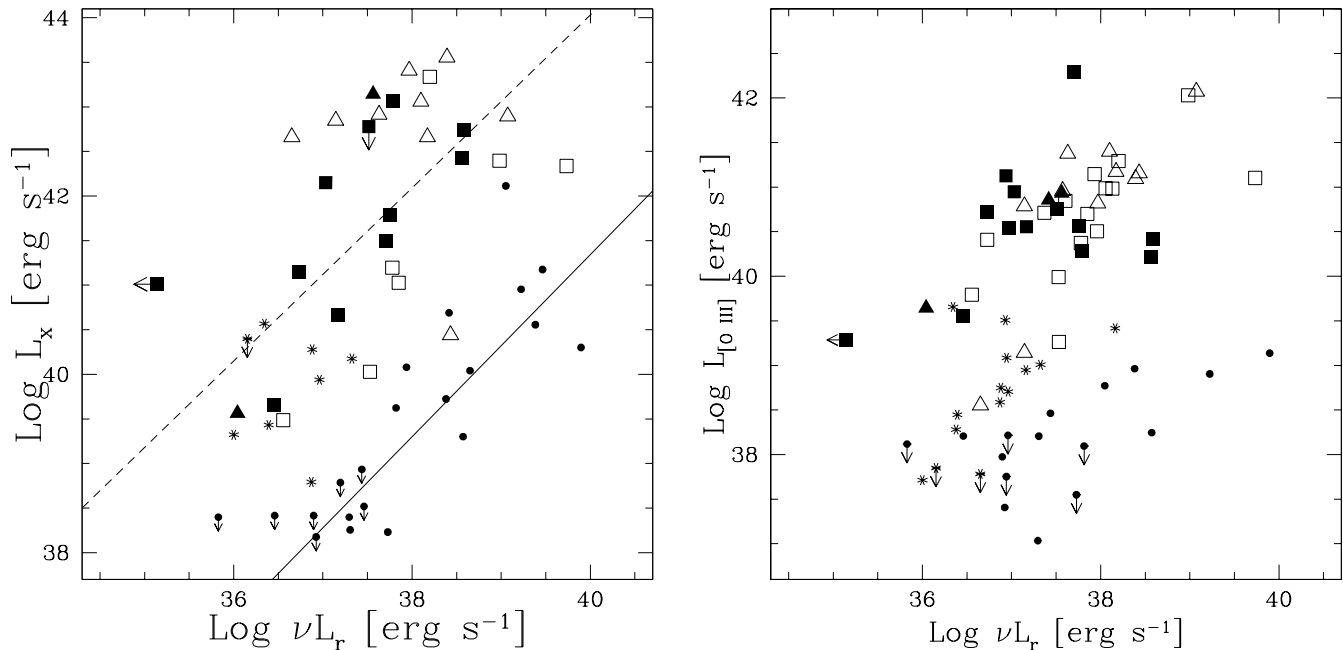


Fig. 6. Left panel: comparison of radio-core (at 3.6 cm) and X-ray nuclear luminosity (in the 2-10 keV band) for the sample of Seyfert galaxies (triangles are Sy 1, squares are Sy 2). Filled symbols represent Seyfert for which it was possible to obtain and fit the brightness profile. We also report “power-law” galaxies (stars) and “core” galaxies (filled circles) from CB06. The solid line represents the correlation derived in BC06 between radio and X-ray nuclear luminosity of radio-loud AGN, including “core” galaxies and the 3C/FR I sample of low luminosity radio-galaxies from Balmaverde et al. (2006). The dashed line represents the same relation derived by Panessa et al. (2007) from their sample of Seyfert galaxies. Right panel: comparison of radio and [O III] emission line luminosity, using the same symbols as in the left panel.

loudness below the threshold of $\text{Log } R_X = -2.8$ derived by Panessa et al. (2007) that provides the best separation between radio-loud and radio-quiet low luminosity AGN. Furthermore, the dichotomy between radio-quiet and radio-loud AGN becomes much stronger with the inclusion of Seyfert galaxies. Indeed, in CB06 we argued that one of our selection criteria for “power-law” galaxies, i.e. the detection of a radio source, was likely to bias the sample toward the inclusion of the radio-quiet AGN with higher radio loudness parameters and that they were likely to represent only the tail, toward high values of R , of the overall population of radio-quiet AGN. This is confirmed by the present analysis.

Our results are based on the sub-sample of objects for which are available HST images suitable for the analysis of the surface brightness profile, representing about one third of the sample. It is then important to assess whether they provide us with an unbiased representation of Seyfert galaxies hosted by early-type galaxies. We therefore considered the distributions of M_{BH} , M_K , of the luminosities in radio, line and X-ray, as well as of the radio loudness parameters R_X and $R_{[OIII]}$. According to the Kolmogorov-Smirnov test, the probability P that the two samples are drawn from the same parent distribution is always larger than 0.80, and the medians differ by at most a factor of 1.3. The only exception is the radio lumi-

nosity (and consequently the spectroscopic radio loudness parameter $R_{[OIII]}$) for which we found $P = 0.38$. This indicates that the objects for which a surface brightness analysis was possible have, on average, a lower radio luminosity. However, the medians of the two distributions ($\text{Log } L_r = 37.2$ and 37.6 respectively) differ only by a factor of 2.5, not a substantial offset considering the range of 4 orders of magnitude in L_r covered by the sample. Conversely, we note that the fraction of objects for which it was possible to perform an isophotal analysis differs drastically from objects imaged in the optical (12%) and in the infrared (67%), mostly likely due to the reduced effects of dust obscuration. Apparently, the strongest influence on the possibility of a successful analysis of the brightness profile is related to the band in which the HST observations were taken, and not to the AGN or host properties. We conclude that the sub-sample of 16 objects with well behaved brightness profiles is well representative of the population of Seyfert hosted in early-type galaxies, with only a slight preference in favor of sources with lower radio emission.

5. Summary and discussion

We presented a study of a sample of 42 nearby ($cz \leq 7000 \text{ km s}^{-1}$) early-type galaxies hosting a Seyfert nu-

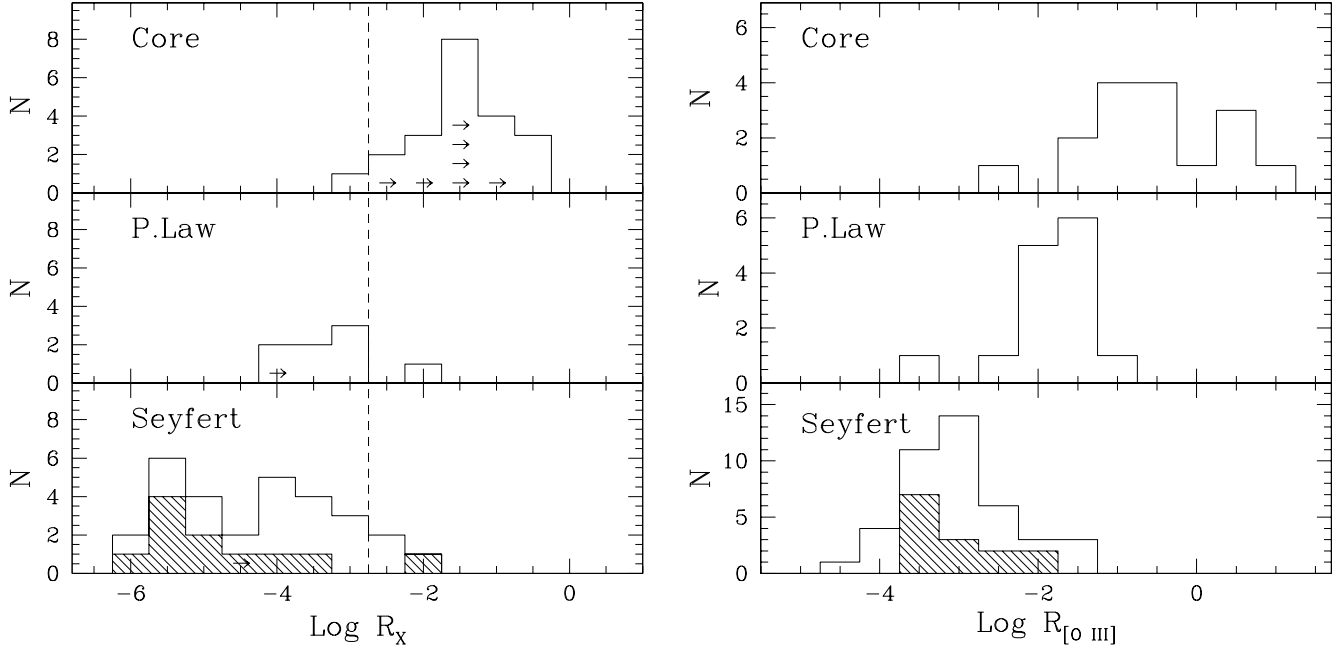


Fig. 7. Left panel: distribution of radio loudness parameter estimated from the ratio of radio and X-ray nuclear luminosity $R_X = (\nu L_r/L_x)$ compared for the two sub-samples of early-type galaxies we analyzed in CB05 (separated into “core” and “power-law” galaxies) and for the present sample of Seyfert galaxies. The shaded region in the bottom panel marks the contribution of type I Seyfert. The vertical dashed line mark the value of R_X that provides the best separation between radio-loud and radio-quiet low luminosity AGN from Panessa et al. (2007). Right panel: same as the left panel, but comparing the spectroscopic radio loudness parameter $R_{[OIII]} = (\nu L_r/L_{[OIII]})$ of the three samples.

cleus. From the nuclear point of view, they show a large deficit of radio emission (at given X-ray or narrow line luminosity) with respect to radio-loud AGN, conforming with their identification with radio-quiet AGN. With only 3 exceptions, their X-ray based radio loudness parameter is smaller than the threshold value of $\text{Log } R_X = -2.8$ introduced by Panessa et al. (2007) to separate radio-loud and radio-quiet low luminosity AGN.

We analyzed their brightness profiles by using archival HST images. Having discarded complex and highly nucleated galaxies we were left with a sub-sample of 16 well behaved objects. By fitting the brightness profiles with a Nukers law, we found that the nuclear cusps are reproduced with a slope in the range $\gamma = 0.51 - 1.07$, typical of “power-law” galaxies.

The lack of “core” galaxies (i.e. galaxies with $\gamma < 0.3$) is not simply the consequence of the luminosity of the Seyfert hosts. In fact, their range of K band absolute magnitudes is $-22.5 < M_K < -25.2$, with only one exception. Adopting a color of $V-K=3.3$ (Mannucci et al. 2001) this translates into $M_V = -19.2 - -21.9$ indicating that most objects lie in the luminosity range where “core” and “power-law” coexist (i.e. $-20 < M_V < -22$, Lauer et al. 2006). Nonetheless, only “power-law” profiles were found from our analysis. Although the reference sample of Lauer et al. is not complete, thus preventing us to assess the significance of this result on a statistical basis, the lack of “core” galaxies as hosts of radio-quiet AGN confirms the presence

of a link between the brightness profile and the AGN radio loudness.

With respect to the initial series of 3 papers we included here a full modeling of the brightness profiles also with a Sérsic model. In no object we found evidence for a central light deficit with respect to a pure Sérsic model, the defining feature of “core” galaxies in this modeling framework. We also assessed that such a light deficit, extending over a fiducial core size of 200 pc, would have been easily seen despite the larger distances of these galaxies (relative to other samples studied in the literature) and the presence of prominent nuclear point sources.

The analysis of the early-type galaxies in the Virgo Cluster Survey presented in Ferrarese et al. (2006) provides us with a useful benchmark for the interpretation of the results obtained from a Sérsic fit of the brightness profiles. In particular, the correspondence we found between the classification as “power-laws” (in the Nukers scheme) and pure-Sérsic galaxies naturally emerges from the inspection of the properties of the Ferrarese et al. sample. Pure-Sérsic galaxies form a well defined sequence in the $\gamma_{0.1}$ vs n plane⁶ (see their Fig. 166, panel bc) with $\gamma_{0.1}$ steadily increasing with n , while “core” galaxies stand aside, forming a well separated group; furthermore, brighter galaxies have larger values of n and, on average, also of $\gamma_{0.1}$ (see their Fig. 166, panels ac and ab). Thus, in

⁶ $\gamma_{0.1}$ is the logarithmic slope of the brightness profile evaluated at $0''.1$, and it corresponds to $\gamma_{0.1} = b_n/n \times (r_e/0.1)^{-1/n}$

the luminosity range of our sample, substantially higher than the average for the VCS, the Sérsic model predicts rather steep central slopes. Indeed, the values of $\gamma_{0.1}$ estimated for the Seyfert hosts (given in Table 3) are in the range 0.36 - 1.02, with a median of 0.48. Not surprisingly their steep cusps are well reproduced by “power-laws” profiles in the Nukers scheme.

Similarly, we have already shown in BC06 that galaxies classified as “core” in the Nuker scheme are reproduced by a core-Sérsic profile, i.e. with a well defined light deficit from a pure Sérsic model. Effectively, when considering relatively bright galaxies (brighter than $\sim M^* + 2$), such as those analyzed here and in our previous papers, there is apparently a complete correspondence between pure Sérsic and “power-law” galaxies on one side, and between core-Sérsic and “core” Nukers galaxies on the other.

It must also be noted that the controversy over the analytical form to be used to reproduce the brightness profiles is not in whether or not there are two classes of early-type galaxies, but in the form of the central structure on the non-core class. In fact, despite their different approaches, Lauer et al. and Ferrarese et al. both identify “core” galaxies as a separate class of objects.

Quite reassuringly, the link between the brightness profile and the AGN radio loudness is independent on the fitting scheme since we recover a unique correspondence between the host’s brightness profile and the AGN properties. Our general results can then be re-phrased as *radio-loud nuclei are hosted by “core” galaxies while radio-quiet AGN are found in “non-core” galaxies*.

In particular, the study presented here enabled us to confirm that radio-quiet AGN are hosted by “non-core” galaxies. The inclusion of Seyfert galaxies extends the coverage up to an X-ray luminosity of $\sim 10^{43}$ erg s $^{-1}$, a factor of 1000 larger than the median luminosity of the sample of radio-quiet AGN we discussed in CB06. Taking the results presented here, in CB06, and in de Ruiter et al. (2005) (where we showed that low-luminosity radio-galaxies are hosted by “core” galaxies), we have covered the different manifestations of nuclear activity in the local Universe. We consistently recovered the association of radio-loud AGN with “core” galaxies and of radio-quiet AGN with “non-core” galaxies. We also confirm that radio-loud and radio-quiet nuclei cannot be distinguished on the basis of other parameters, such as the host’s luminosity or the black-hole mass, as they differ only on a statistical basis. In particular Seyfert hosts reach an absolute magnitude of $M_K \sim -25$ and harbor black holes with masses as high as $4 \times 10^8 M_\odot$, well into the range of radio-loud AGN. Only the brightness profiles provide a full separation between the two classes.

References

Awaki, H., Ueno, S., Taniguchi, Y., & Weaver, K. A. 2000, ApJ, 542, 175
 Balmaverde, B. & Capetti, A. 2006, A&A, 447, 97 (BC06)

Balmaverde, B., Capetti, A., & Grandi, P. 2006, A&A, 451, 35
 Capetti, A. & Balmaverde, B. 2005, A&A, 440, 73 (CB05)
 Capetti, A. & Balmaverde, B. 2006, A&A, 453, 27 (CB06)
 Cappi, M., Bassani, L., Comastri, A., et al. 1999, A&A, 344, 857
 Chiaberge, M., Capetti, A., & Macchetto, F. D. 2005, ApJ, 625, 716
 Croton, D. J., Springel, V., White, S. D. M., et al. 2006, MNRAS, 365, 11
 de Ruiter, H. R., Parma, P., Capetti, A., et al. 2005, A&A, 439, 487
 Di Matteo, T., Springel, V., & Hernquist, L. 2005, Nature, 433, 604
 Dunlop, J. S., McLure, R. J., Kukula, M. J., et al. 2003, MNRAS, 340, 1095
 Durret, F. & Bergeron, J. 1986, A&A, 156, 51
 Fabbiano, G., Kim, D.-W., & Trinchieri, G. 1992, ApJS, 80, 531
 Faber, S. M., Tremaine, S., Ajhar, E. A., et al. 1997, AJ, 114, 1771
 Feldmeier, J. J., Brandt, W. N., Elvis, M., et al. 1999, ApJ, 510, 167
 Ferrarese, L., Côté, P., Jordán, A., et al. 2006, ApJS, 164, 334
 Ferrarese, L. & Merritt, D. 2000, ApJ, 539, L9
 Ferruit, P., Wilson, A. S., & Mulchaey, J. 2000, ApJS, 128, 139
 Gebhardt, K., Bender, R., Bower, G., et al. 2000, ApJ, 539, L13
 Graham, A. W., Erwin, P., Trujillo, I., & Asensio Ramos, A. 2003, AJ, 125, 2951
 Graham, A. W. & Guzmán, R. 2003, AJ, 125, 2936
 Gu, Q., Melnick, J., Fernandes, R. C., et al. 2006, MNRAS, 366, 480
 Häring, N. & Rix, H.-W. 2004, ApJ, 604, L89
 Hewitt, A. & Burbidge, G. 1991, ApJS, 75, 297
 Ho, L. C., Filippenko, A. V., & Sargent, W. L. W. 1997, ApJS, 112, 315
 Ho, L. C. & Peng, C. Y. 2001, ApJ, 555, 650
 Jędrzejewski, R. I. 1987, MNRAS, 226, 747
 Kellermann, K. I., Sramek, R. A., Schmidt, M., Green, R. F., & Shaffer, D. B. 1994, AJ, 108, 1163
 Khochfar, S. & Burkert, A. 2003, ApJ, 597, L117
 Koski, A. T. 1978, ApJ, 223, 56
 Kriss, G. A., Canizares, C. R., & Ricker, G. R. 1980, ApJ, 242, 492
 Kuraszkiewicz, J., Wilkes, B. J., Brandt, W. N., & Vestergaard, M. 2000, ApJ, 542, 631
 Lauer, T. R., Ajhar, E. A., Byun, Y.-I., et al. 1995, AJ, 110, 2622
 Lauer, T. R., Gebhardt, K., Faber, S. M., et al. 2006, ApJ submitted, astro-ph/0609762
 Levenson, N. A., Weaver, K. A., & Heckman, T. M. 2001, ApJS, 133, 269
 Maiolino, R., Salvati, M., Bassani, L., et al. 1998, A&A, 338, 781
 Malaguti, G., Bassani, L., Cappi, M., et al. 1999, A&A,

- 342, L41
- Mannucci, F., Basile, F., Poggianti, B. M., et al. 2001, MNRAS, 326, 745
- Maoz, D. 2007, astro-ph/0702292
- Marconi, A. & Hunt, L. K. 2003, ApJ, 589, L21
- Matt, G., Bianchi, S., Guainazzi, M., et al. 2003, A&A, 399, 519
- Milosavljević, M., Merritt, D., Rest, A., & van den Bosch, F. C. 2002, MNRAS, 331, L51
- Molendi, S., Maccacaro, T., & Schaeidt, S. 1993, A&A, 271, 18
- Mulchaey, J. S., Koratkar, A., Ward, M. J., et al. 1994, ApJ, 436, 586
- Mulchaey, J. S., Wilson, A. S., & Tsvetanov, Z. 1996, ApJS, 102, 309
- Murayama, T. & Taniguchi, Y. 1998, ApJ, 497, L9+
- Nagar, N. M., Wilson, A. S., Mulchaey, J. S., & Gallimore, J. F. 1999, ApJS, 120, 209
- Nelson, C. H. & Whittle, M. 1995, ApJS, 99, 67
- O'Brien, P. T., Page, K., Reeves, J. N., et al. 2001, MNRAS, 327, L37
- Panessa, F., Barcons, X., Bassani, L., et al. 2007, astro-ph/0701546
- Pfefferkorn, F., Boller, T., & Rafanelli, P. 2001, A&A, 368, 797
- Ravindranath, S., Ho, L. C., & Filippenko, A. V. 2002, ApJ, 566, 801
- Reynolds, C. S. 1997, MNRAS, 286, 513
- Risaliti, G., Elvis, M., & Nicastro, F. 2002, ApJ, 571, 234
- Roberts, T. P. & Warwick, R. S. 2000, MNRAS, 315, 98
- Ryden, B. S., Forbes, D. A., & Terlevich, A. I. 2001, MNRAS, 326, 1141
- Sérsic, J.-L. 1968, Atlas de Galaxias Australes(Córdoba: Obs. Astron.)
- Shuder, J. M. 1980, ApJ, 240, 32
- Shuder, J. M. & Osterbrock, D. E. 1981, ApJ, 250, 55
- Storchi Bergmann, T. & Pastoriza, M. G. 1989, ApJ, 347, 195
- Terashima, Y., Ho, L. C., Ptak, A. F., et al. 2000, ApJ, 533, 729
- Terashima, Y., Iyomoto, N., Ho, L. C., & Ptak, A. F. 2002, ApJS, 139, 1
- Terashima, Y. & Wilson, A. S. 2003, ApJ, 583, 145
- Tremaine, S., Gebhardt, K., Bender, R., et al. 2002, ApJ, 574, 740
- Trujillo, I., Erwin, P., Asensio Ramos, A., & Graham, A. W. 2004, AJ, 127, 1917
- Turner, T. J., George, I. M., Nandra, K., & Mushotzky, R. F. 1997, ApJS, 113, 23
- Ulvestad, J. S. & Wilson, A. S. 1983, AJ, 88, 253
- Veron-Cetty, M.-P. & Veron, P. 1991, European Southern Observatory Scientific Report, 10, 1
- Whittle, M. 1992, ApJS, 79, 49
- Whittle, M., Pedlar, A., Meurs, E. J. A., et al. 1988, ApJ, 326, 125
- Wilson, A. S. & Colbert, E. J. M. 1995, ApJ, 438, 62
- Wilson, A. S., Wu, X., Heckman, T. M., Baldwin, J. A., & Balick, B. 1989, ApJ, 339, 729